We are IntechOpen, the world's leading publisher of Open Access books
Built by scientists, for scientists

4,800
Open access books available

122,000
International authors and editors

135M
Downloads

Our authors are among the

154
Countries delivered to

TOP 1%
most cited scientists

12.2%
Contributors from top 500 universities

CLARIVATE ANALYTICS
BOOK CITATION INDEX
INDEXED

WEB OF SCIENCE™

Selection of our books indexed in the Book Citation Index in Web of Science™ Core Collection (BKCI)

Interested in publishing with us?
Contact book.department@intechopen.com

Numbers displayed above are based on latest data collected.
For more information visit www.intechopen.com

7

Self-Assembled InAs(N) Quantum Dots Grown by Molecular Beam Epitaxy on GaAs (100)*

Alvaro Pulzara-Mora[1], Juan Salvador Rojas-Ramírez[2], Victor Hugo Méndez García[3], Jorge A. Huerta-Ruelas[4], Julio Mendoza Alvarez[2] and Maximo López López[2]

[1]*Laboratorio de Magnetismo y Materiales Avanzados, Universidad Nacional de Colombia Sede Manizales;*

[2]*Physics Department, Centro de Investigación y Estudios Avanzados del IPN, México D.F., México;*

[3]*Coordinación para la Innovación y Aplicación de la Ciencia y Tecnología, Universidad Autónoma de San Luis Potosí, San Luis Potosí, S.L.P, México*

[4]*Centro de Investigación en Ciencia Aplicada y Tecnología Avanzada, Instituto Politécnico Nacional Cerro Blanco 141 Colinas del Cimatario Querétaro, Querétaro México México*

1. Introduction

The zero-dimensional nature of self-assembled quantum dots (SAQDs) is of great interest for high-performance optoelectronic devices such as semiconductor lasers [Kita et al., 2003]. Self-assembled Stranski–Krastanov (SK) growth mode is a promising technique to realize defect free and high SAQDS density. However, the size fluctuations of SAQDS observed in SK growth mode hinder the realization of devices superior performance.

The device performance strongly depends on the SAQDs parameters, such as the size, density, and uniformity, which can be controlled by performing precise growth. Most studies on SAQDs have been focused on InAs/GaAs systems and toward developments in optical fiber communication systems at wavelengths of 1.3 or 1.55 μm [Matsuura et al, 2004; A. Ueta et al, 2004]. However, it is difficult to obtain emissions in this wavelength region with InAs SAQDs, because of the strain effects inside them. InAs has a large lattice mismatch (~7%) to GaAs, and InAs SAQDs embedded inside structures are strongly compressed by their surrounding GaAs barriers. Recently, dilute nitride III–V compounds have been the subject of important research interest as they exhibit new properties that are potentially useful for narrow band gap devices. It has been found that replacing a small amount (< 5%) of the group V element by nitrogen in III–V compounds reduces the energy gap and changes the electronic structure, such as InAsN alloy due to its large bowing factor (b≈16) [J. Wu et al, 2002], thus offering new perspectives for band structure engineering in order to improve optoelectronic properties. Therefore, InAsN SAQDs are promising to obtain emissions at a wavelength of 1.55 μm and longer [L. Ivanova et al, 2008].

On the other hand, it is widely known that reflection high-energy electron diffraction (RHEED) is a powerful in-situ characterization technique, RHEED is quite sensitive to the

crystallographic surface structures in real time. Many authors have used this technique to study the QD shape evolution during the GaAs capping layer growth. However, very few authors have studied the relation between diffraction pattern (chevrons) with the shape and size of quantum dots [H. Lee et al, 1998; T. Hanada et al, 2001b]. In order to minimize the effects of size and shape fluctuation, the growth parameters such as growth temperature and Arsenic overpressure must be optimized.

On the other hand, in a similar way as in GaAsN and GaPN alloys, the incorporation of Nitrogen (N) in InAs, yields a large bandgap bowing which produces a significant reduction of the bandgap energy. Therefore, InAsN SAQDs are promising to obtain emissions at a wavelength of 1.55 μm and longer.

In this work we have studied the effects of growth temperature and Arsenic overpressure on the growth mode of InAs(N) SAQDs on GaAs(100) substrates. The wavelength emission of the InAs(N) SAQDs was evaluated depending on growth conditions. We present an analysis of the asymmetric broadening of the Raman spectra using the confinment phonon model (CM).

2. Experimental

The SAQDs were grown on GaAs (100) substrates employing a Riber C21 MBE system equipped with solid sources for III-V materials, and standard reflection high-energy electron diffraction (RHEED) system. For structures requiring Nitrogen Atomic Nitrogen was produced by a radio frequency (RF) plasma source. Ultrahigh purity nitrogen was introduced into the plasma source using a mass flux controller and a leak valve. First, in the MBE chamber the substrates were heated up to 580 °C to remove the surface oxides under an As_4 flux. Then, in order to smooth out surface imperfections, a 500nm-GaAs buffer layer was grown at 580 °C. At the end of the buffer layer growth the surface exhibited a sharp (2x4) RHEED pattern. After the buffer layer growth, the temperature was gradually lowered to the desired value (between 480 and 510 ^{o}C) and InAs SAQDs deposition was initiated. At these substrate temperatures the GaAs surface reconstruction changed to a c(4x4). The InAs growth rate was 0,06 monolayer (ML) per second. The growth mode was in-situ monitored by RHEED. Different InAs SAQDs samples were grown by changing the growth temperature, but maintaining constant the fluxes of As_4 and In. For InAsN SAQDs growth the radio frequency plasma source was operated at 100 W with a Nitrogen flux of 0.1 sccm. The InAs SAQDs dimensions and density were determined by Atomic Force Microscopy (AFM) and High Resolution Scanning Electron Microscopy (HRSEM). Photoluminescence Spectroscopy (PL) measurements were carried out at 10 K by using a double monochromator, and an InGaAs cooled detector. The 488 nm line from an Argon laser was used as the excitation wavelength at a 120 mW excitation power.

The structural properties of the samples were studied by micro Raman spectroscopy at room temperature using a spot size of 2x2μm^2, and employing the 632.8nm line of a He–Ne laser in a backscattering configuration.

3. Results and discussion

3.1.1 RHEED Pattern

The temporal evolution of the RHEED intensity variation of the transmission spot for the InAs SAQDs grown at substrate temperatures of (M1) 480 ^{o}C, (M2) 490 ^{o}C, and (M3) 510

ºC, with identical Arsenic overpressure (3x10-7Torr), are shown in Fig. 1. During the first stages of InAs deposition a small hump was observed in the RHEED intensity, then it decreased smoothly. Finally, the RHEED intensity rises until reaching a saturation value. The RHEED patterns changes were continuously monitored from the wetting layer formation to the nucleation of self-assembled InAs dots. The RHEED pattern taken along the [01-1] azimuth from the buffer layer just at the start of InAs growth (marked by a downwards dashed arrow in Fig. 1) showed a c(4x4) GaAs surface reconstruction. Streaky RHEED patterns were maintained during the wetting layer formation (time t_{2D} in Fig. 1) indicating a layer by layer growth (the end of t_{2D} is marked by the downwards arrows in Fig. 1). However, after the elapsed time t_{2D} of InAs deposition, the streaky RHEED patterns changed to spotty, and the so-called Chevron patterns were evidenced [J.W. Lee et al, 2004], indicating the formation of 3D-dimensional structures.

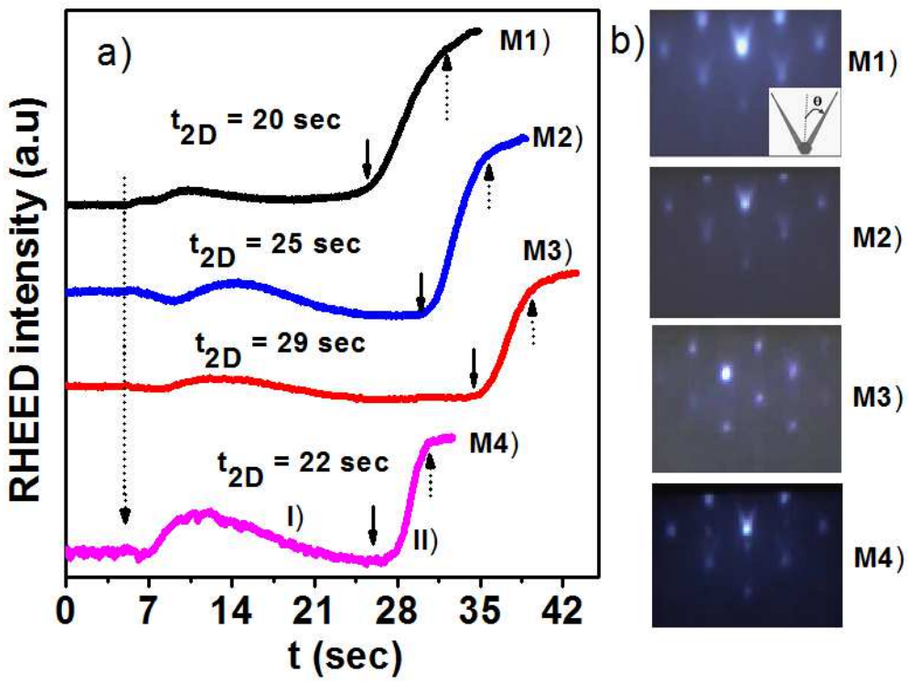

Fig. 1. (a) RHEED intensity of the transmission spot as a function of growth time (t) for InAs SAQDs grown at temperatures of: (M1) 480 ºC, (M2) 490 ºC, (M3) 510 ºC, and (M4) 510 ºC with Nitrogen. (b) RHEED patterns along the [01-1] after the growth of the InAs SAQDs. A constant Arsenic overpressure of 3x10-7 Torr was employed in all the growths.

The Chevron patterns consists of two well defined wings with an angle to each other of 2θ = 50 º and 2θ = 56 º for sample M1 and M2, respectively, as shown in the right column of Fig. 1. The fact that the Chevron´s angle increases by increasing the growth temperature, indicates that the slope of the facets that limit the SAQDS tends to increase with increasing growth temperature. The self-assembling process during the MBE growth is a non-equilibrium process, which is controlled by particular kinetics of diffusion and nucleation dependent on the growth conditions and the thermodynamics of the surface. The interplay of both, determines the ultimate morphology of the quantum dots, i.e., the facets that surround them. Nevertheless, in MBE growth usually the kinetic constrains seem to be

predominant on the role of the intrinsic surface free energy. The change of the islands facets slope could be a result of an increase of the surface diffusion of In adatoms on the surface. For sample M3 the Chevron patterns are not well defined, rounded spots are observed similar to those present when the facets have the {163} crystal plane orientation.

In order to analyze the nitridation effects on InAs SAQDs formation, we grew an InAsN sample (M4) under identical conditions as for the sample M3 (T_g = 510 °C), but in a Nitrogen overpressure of $2x10^{-5}$ Torr. This temperature was employed in order to incorporate a low nitrogen content into the InAs SAQDs [A. Pulzara-Mora et al, 2007]. The RHEED intensity variation of the transmission spot for sample M4 (Fig. 1.) presented a similar behaviour as that for the InAs samples (M1-M3). However, the growth time for wetting layer formation (t_{2D}) decreases showing the strong effects of nitrogen incorporation into the SAQDs. Moreover, the Chevrons of RHEED patterns for sample M4 taken at the end of growth are better defined than those for sample M3, with a Chevron's angle of 2θ = 47.2°. The decrease of the Chevron's angle for sample M4 can be considered due to a decrease in the In surface diffusion caused by the additional Nitrogen overpressure. Note that a similar result has been observed when using a high Arsenic overpressure for the InAs QDs growth [T. Kudo et al, 2008]. These results suggest that the geometry and size of SAQDs can be changed by introducing Nitrogen during the InAs growth. We will discuss this point in the SEM and AFM images section.

Sample	Growth temperature (°C)	Angle (2θ) (degrees)	Facet planes
M1	480	49.84	(113)
M2	490	55.74	(113) tilted to (112)
M3	510	-	(136)
M4 (with Nitrogen)	510	47.2	(113) tilted to (114)

Table 1. Angle (2θ) of the Chevrons of RHHED patterns and the associated facet planes.

In table I we summarize the Chevron's angle (θ) in the RHEED patterns of SAQDs grown under different conditions, and the associated crystal planes of the facets. The corresponding (1 1 x) planes of the facets were obtained from the linear correlation between the tangent of the Chevron semi-angle θ/2 and the magnitude of the index x [A. Feltrin et al, 2007]. We found that

$$tan\left(\frac{\theta}{2}\right) = \frac{\sqrt{2}}{x} \quad (1)$$

3.1.2 Morphological characterization

Fig. 2 (I), shows a HRSEM image taken in cross-section view (x 300000) from sample M4. In this image is clearly observed the substrate (S), buffer layer (BL) and semi-spherical shaped SAQDs nucleated on the wetting layer. The InAs SAQDs have a height between 7 and 10 nm. The HRSEM image of the same sample in Fig. 4 (II) taken in plane view (x50000), shows that the SAQDs are not homogeneously distributed on the wetting layer, but they tend to nucleate on preferential regions. We think that those regions are surface steps on the GaAs (100) substrate [S. O. Cho et al, 2006], as illustrated in the sketch inserted in the micrograph.

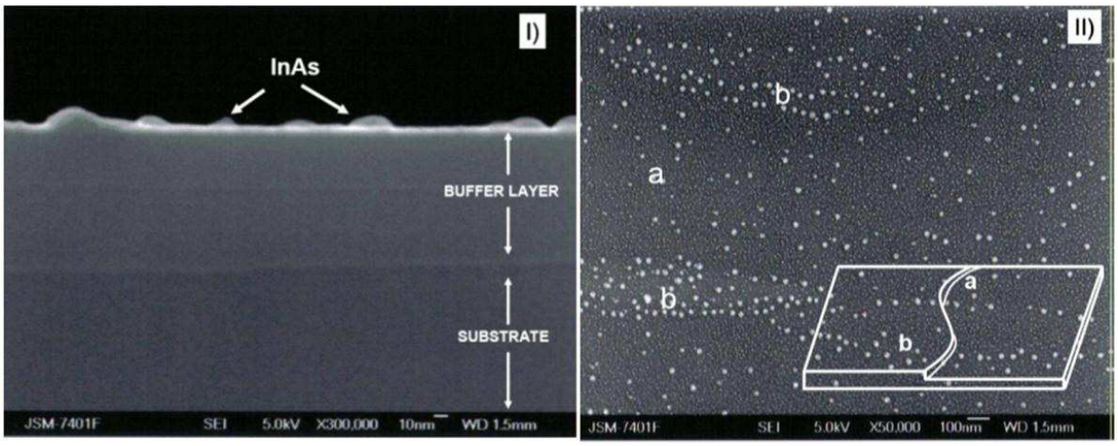

Fig. 2. (I) Cross-sectional HRSEM image (x300.000) of InAs SAQDs. (II) Plane view HRSEM image (x50.000) of InAs SAQDs. The inset shows schematically the preferential sites for SAQDs nucleation.

AFM images with a scanned area of 1×1 μm² of InAs dots on the (100) GaAs surface are shown in Figs. 3 (M1-M3). The dot densities obtained from a statistical analysis are: 6.84×10^{10} cm^{-2}, 3.4×10^{10} cm^{-2} and 1.87×10^{10} cm^{-2}, for M1, M2 and M3, respectively. We also observe that the average InAs dots size tends to increase with increasing the growth temperature, this could be due to an increase in the surface mobility of In adatoms [M. Sopanen et al, 2000; S. Kiravitaya et al, 2002]. On the other hand, the density of the InAsN SAQDs was 8.7×10^{9} cm^{-2}. By comparing the AFM images for samples M3 and M4, we observed that the density of InAsN SAQDs is one order of magnitude lower than that of sample M3 grown under identical Arsenic overpressure and substrate temperature. Moreover, we noted that the nitridation of InAs SAQDs promoted the formation of quantum dots of larger dimensions (≥10 nm).

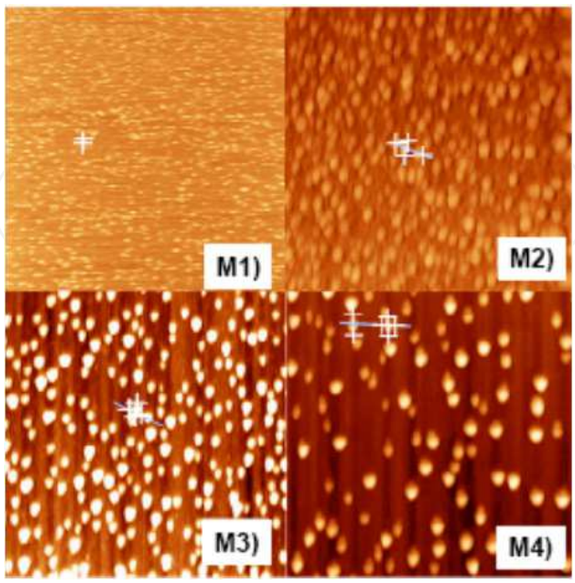

Fig. 3. 1x1 μm² AFM images of InAs SAQDs (M1, M2, and M3) and InAsN SAQDs (M4).

3.2 Optical characterization

Among the optical methods to characterize epitaxially grown quantum dots, photoluminescence and Raman spectroscopy are probably the most common. We used these techniques to find out the ground state transition of the InAs SAQDs, and analyzed the possible phonon scattering come from GaAs, InAs QDs, and surface phonon modes. All photoluminescence spectra were taken at 10 K. The Raman spectra were taken at room temperature by using a backscattering configuration.

3.2.1 Photoluminescence (PL)

In photoluminescence (PL), when a quantum dot is irradiated with light, a photon with energy $h\omega_{exc}$ is absorbed in the quantum dot or in the surrounding material, creating an electron-hole pair (excitation). Then, electron and hole is relaxed by moving to the energetically lowest state in the QD (relaxation).

The relaxation process for the electrons is through the creation of phonons, which have quantized energies. This effect known as phonon bottleneck has been reported for various authors [H. Benisty et al, 1981; R. Heitz et al, 2001]. Finally, the electron-hole pair recombines, emitting a photon with energy $h\omega_{rec}$ (recombination) which is detected as PL light. Fig. 4 shows the schematic representation of the PL process in a quantum dot. On the other hand, due to the incident light spot in the PL experimental setup is much larger than 1 μm^2, many QDs are excited simultaneously. Therefore, several series of peaks can be observed simultaneously, which result in one broad peak as shown by the experimental PL results. In a quantum dot the single particle energies of electrons or holes depend almost solely on the QD's structural properties like size, shape, composition and the surrounding material.

The single particle picture is, however, no longer sufficient if a QD is occupied by more than one charge carrier, because the Coulomb interaction between the confined particles alters the overall energy of the system. For bulk and quantum well structures this well-known effect is referred to as renormalization of the band gap. For fully confined systems like QDs such renormalization is also expected to play a role but to have only minor impact, since the strong confinement dominates the electronic properties of a QD.

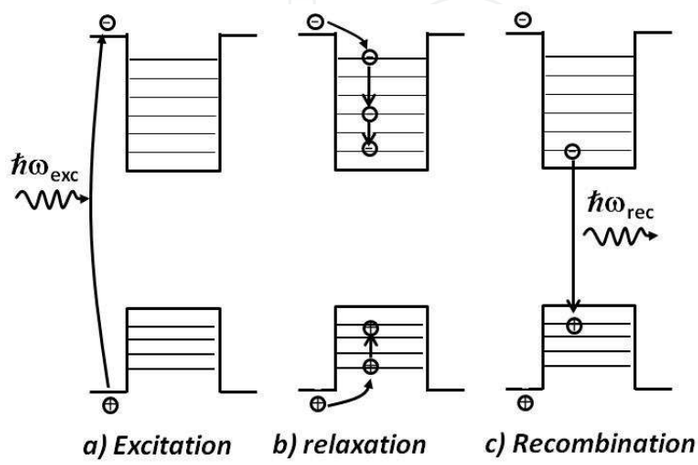

Fig. 4. Schematic representation of the photoluminescence processes in a Quantum dot

The PL band is the convolution of all the emission lines of every single QD which is excited; the lines have an homogenous broadening, due to optical recombination and scattering by phonons and impurities, and an inhomogenous one, related to differences in size, shape and composition of individual QDs. Therefore, the shape of the PL bands reflects the distribution of quantum confined energy levels in QDs [S. Franchi et al, 2003].

PL spectrum for the InAs and InAsN SAQDs are shown in Fig. 5(a). PL spectrum for the InAs and InAsN SAQDs are shown in Fig. 4(a). The PL spectra for the samples M1-M3 show a broad (100, 86, and 81 meV, respectively), symmetric main peak, coming from the statistical distribution of SAQDs. The position of the PL peak varies from the 1.23 μm to 1.52 μm depending on InAs SAQDs sizes. Great efforts have been made to obtain SAQDs emitting at longer wavelengths for a variety of applications. One possibility is to make an annealing on the samples in an ultra high vacuum atmosphere [O. Suekane et al, 2002], another possibility is to carry out a nitridation of InAs SAQDs after growth. However, the crystalline quality of the InAs dots is degraded, and the optical properties change drastically. Therefore, we preferred to carry out the nitridation during the InAs growth (sample M4). In this case the optical quality of the InAsN SAQDs didn't present considerable changes as can be seen in Fig. 5(a) (M4). The PL signal for sample (M4) has a long asymmetric tail at short wavelengths, probably due to incorporation of atoms or clusters of Nitrogen in the InAs SAQDs typical of III-V:N compounds [V. Sallet et al, 2005]. The PL peak of sample M4 is located at 1.55 μm, this red-shift could be caused by the following effects: 1) Nitrogen incorporation in the wetting layer, which decreases the compressive stress because $a_{InAs}>a_{InAsN}>a_{GaAs}$, where a_{InAs}, a_{InAsN}, and a_{GaAs} are the InAs, InAsN and GaAs lattice parameters, respectively. 2) Nitrogen incorporation in the SAQDs, as above mentioned the bandgap of III-V compounds is reduced by the incorporation of N. 3) The formation of larger SAQDs promoted by the incorporation of Nitrogen as observed in AFM images presented in the Fig. 4 (M4).

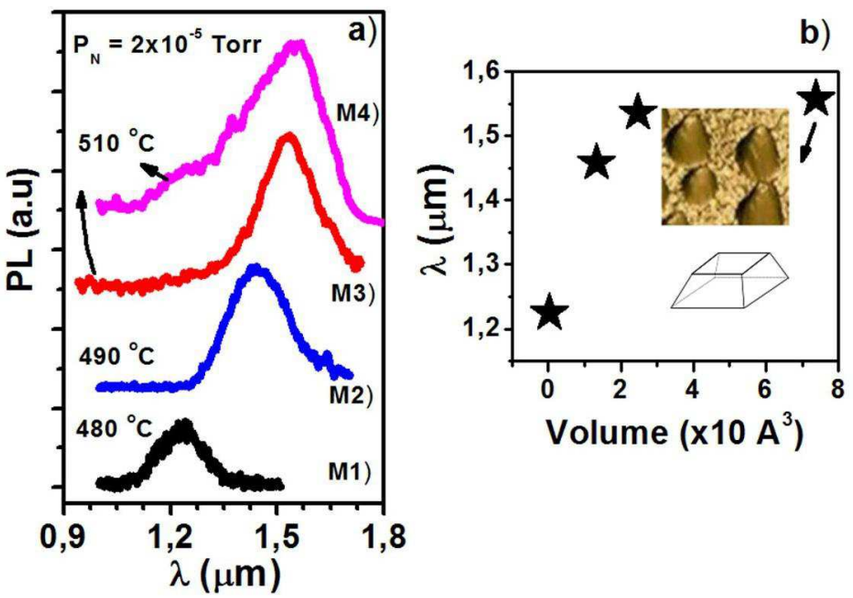

Fig. 5. (a) Low temperature PL spectra of InAs (M1, M2 and M3) and InAsN (M4) SAQDs. (b) Wavelength emission as a function of the SAQDs volume.

The PL peak position for the InAs(N) SAQDs is shown in Fig. 5(b) as a function of dots volume obtained from AFM measurements, and by using the geometry of a truncated pyramidal solid as it is shown in the inset of this figure. The wavelength of the PL emission increases for larger InAs SAQDs as a consequence of decreasing the quantum confinment.

3.2.2 Raman Spectroscopy (RS)

Raman spectroscopy on solids is nowadays widely known as a means of studying phonons, while it is also a very suitable method to study electronic collective excitations in semiconductors nanostructures, such as quantum wells or quantum dots. In the formation of SAQD, it is well known that strain plays an important role and Raman measurement is a strong tool to study strain. The mismatch of lattice constants gives rise to strain fields in QD nanostructures, which will affect their optical properties [L. B. Freund, 2000]. In-plane lattice mismatch parameters are defined as:

$$(\varepsilon_0)_{xx} = (\varepsilon_0)_{yy} = \frac{a_s - a_d}{a_d} \quad (1)$$

Where a_s and a_d are the lattice constants of the substrate (GaAs) and the dot (InAs) materials, respectively, which will be taken as 0.565 and 0.605 nm in this paper. Obviously, the lattice constant of the dot material (InAs) exceeds that of the substrate material (GaAs). Hence, it is expected that InAs will experience compression from GaAs, while GaAs will experience tension from InAs. Note that the lattice mismatch parameters defined in equation (1) do not describe completly strain fields in the quantum-dot island. In fact, lattice mismatches will induce elastic deformation in both the substrate and the island, to ensure the equilibrium of the corresponding stresses.

The evolution of the Raman FWHM and frequency shifts with increasing the QDs zise can also be described by a phenomenological model, the so-called "Phonon Confinement Model" (PCM). This model was originally developed to describe the evolution of the Raman spectra of disordered semiconductors [H. Richter et al, 1981; Tiong et al, 1984]. Later Campbell and Fauchet generalized this model to study the phonon confinement in nanostructures and thin films [I. H. Campbell, 1986]. PCM is widely used method in modeling Raman spectra of low dimensional systems such as quantum wells, quantum wires and quantum dots. Many experimental groups have used the PCM method to explain the observed asymmetry of the one-phonon bands appearing in their nanowire Raman spectra [K. W. adu et al, 2005; Giuseppe Faraci et al, 2006]. However, this method has not been explored in detail for analyzing Raman spectra of InAs SAQDs grown by MBE. We will discuss this point in detail in the next section.

In the phenomenological phonon confinement model (PCM), the Raman scattering intensity I(ω,d) for a spherical particle of diameter L, and Gaussian confinement function is given by [M. Grujic et al, 2009]

$$I(\omega) = I_0 \int_{BZ} |C(o,q)|^2 F[\omega_i(q), \Gamma] d^3q \quad (2)$$

where $|C(o,q)|^2 = e^{-\frac{q^2 L^2}{2\beta^2}}$ is the Fourier coefficient of the confinement enveloped function $W(r) \propto e^{-\left[\frac{\alpha r}{L}\right]^2}$ for the zone centre optical phonon, q is the wave vector $\left[\frac{-\pi}{a} \leq q_{BZ} \leq \frac{\pi}{a}\right]$, a is the

unit cell lattice parameter, and L is the average diameter. The confinement factor β initially was taken as a constant factor (Richter *et al*, β = 1, Campbell *et al*. β = 2π²). However, many authors consider that the confinement factor β must be a fitting parameter in Raman spectra, because it can be dependent on confinement boundary conditions in nanomaterials. $F[\omega_i(q),\Gamma]$ is the spectral line shape related to phonon disperse curve $\omega_i(q)$ with Γ natural line width (FWHM). Gaussian or Lorentzian are the most used lineshapes to fitting the experimental Raman data. However, due to the asymmetry and broadening of our experimental Raman spectra we chosen the so called Breit –Wigner-Fano (BWF) lineshape [Ugo Fano, et al, 1961], given as,

$$F[\omega_i(q),\Gamma] = \frac{Io\left[f\left[\frac{\Gamma}{2}\right]^2+\omega_i(q)-\omega_{LO}\right]^2}{[\omega_{LO}-\omega_i(q)]^2+\left[\frac{\Gamma}{2}\right]^2} \quad (3)$$

In which 1/f is the Fano parameter, and represents the asymmetry of the shape, while Io and Γ are fitting parameters of the intensity and broadening factor, respectively. The Fano line shapes evolve to Lorentzian line when f tends to zero. In the Eq (2), the infinitesimal elemental d^3q volume can be written as q^2dq if a spherical symmetry is considered.

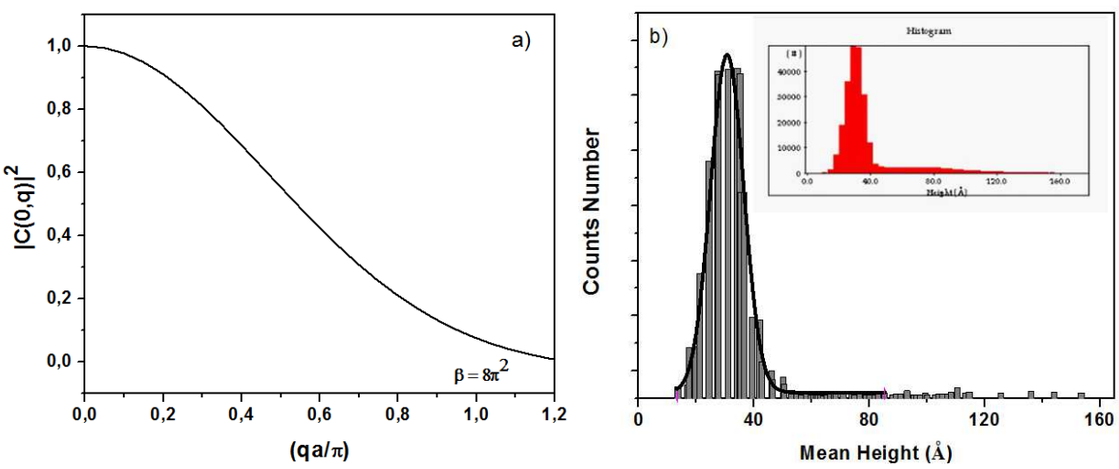

Fig. 6. (a) Squares of the Fourier transform $|Q(0,q)|^2$ used in the confinement phonon model (CM), β = 8π². (b) Diameter distribution of the InAs Qdots (M4-sample) with mean height L = 35 Å. The solid curve is a log-normal fit to the distribution. The inset in (b) is the histogram of the sample M4.

GaAs has two atoms in the unit cell and, therefore, six phonon branches. Three acoustic and three optical. From the three optical branches, one gives rise to an infra-red active mode at the Γ point, while the two other branches are degenerate at the Γ point and Raman active. Therefore, zone center (q = 0) phonons would generate a one peak Raman spectra. However, the electronic structure of GaAs generates special electron-phonon induced resonance conditions with non-zone center modes (q ≠ 0), and the previous rule is not valid. In this case, for the LO phonon frequency dispersion, we can use the diatomic linear-chain model, which is expressed as,

$$\omega(q) = C\sqrt{\frac{M_1+M_2\sqrt{M_1^2+M_2^2+2M_1^2M_2^2\cos(qa)}}{M_1M_2}} \quad (4)$$

where M1 and M2 are the atomic masses of Ga and As, respectively and C is the fitting parameter. (a_{GaAs} = 0.5466 nm).

Fig. 7 shows the Raman spectra taken at room temperature by using the 632 nm excitation laser line. The two peaks at 265 and 290 cm^{-1} are due to scattering from the GaAs TO and LO phonons [Tomoyuki Sekine et al, 2002], respectively. Since Raman measurement is performed in backscattering configuration from (001) growth surface, TO mode should be forbidden. The low intensity of TO mode is due to the departure from the perfect backscattering geometry. It is observed that the line center of these peaks remains practically the same in all the samples. However, by comparing all spectra one can see that the peak position of the TO and the LO peaks are up-shifted about 4.7 cm^{-1} compared with the bulk (001) GaAs (TO = 260 cm^{-1}, LO = 290 cm^{-1}). The compressive stress acting on the QDs can produce produce a blue-shift in the LO-phonon frequency. Presumably, the red-shift induced by phonon confinement compensates for the blue-shift due to the surface pressure effects entirely as has been observed in some semiconductors materials [Campbell I.H. & Fauchet P.M., 1986], embedded in a glass matrix.

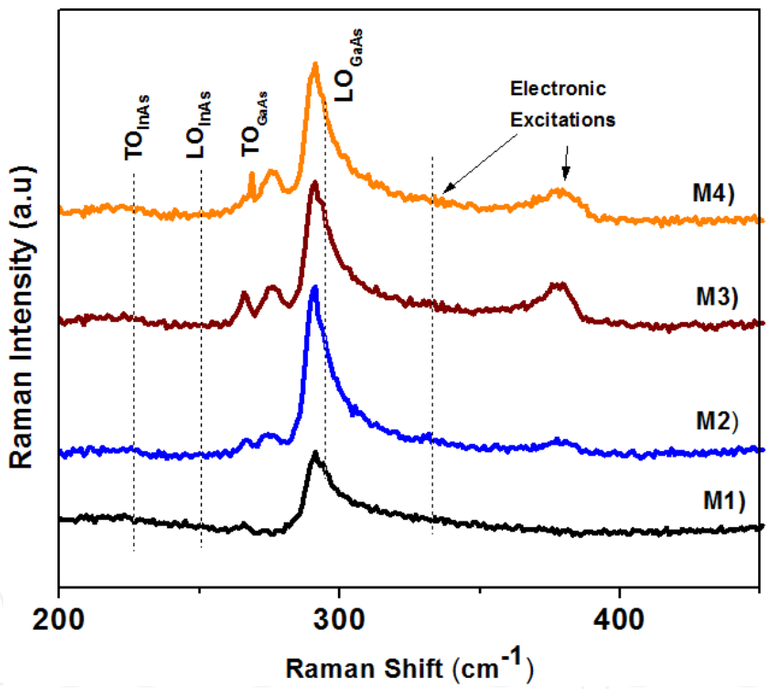

Fig. 7. Raman spectra taken at room temperature of the InAs QDots

On the other hand, it is also observed that the GaAs LO mode is asymmetrically broadened compared to the bulk, as shown the Fig. 6). The asymmetry observed in the one phonon LO Raman has been tentatively assigned to several factors such as particle size distribution, random variations in the bond wave number, and particle shape irregularity [AkhileshK et al, 2007]. Quantum confinement effect can contribute to the asymmetrical broadening observed in the one-phonon LO Raman (Fig 7. and Fig. 8.).

Experimental results show that as the QD volume increases (samples M1 to M4), there is a change in the line shape and full-width at half-maxima (FWHM) of the LO-phonon peaks.

The Raman peak of M4 sample with quantum dots of 73Å^3 volume, has an FWHM of 8.2 cm^{-1}. As the QD volume decreases from 2.4 Å^3 to 0.26 Å^3 the FWHM increases to ≈ 9.8 cm^{-1}. The peak profile is almost symmetric in the case of sample M4, whereas a small asymmetry in the line shape becomes noticeable for the samples in the strongly confined regimen. This observation is more evident for sample M1 with the smallest SAQDs volume

In order to analyze the asymmetry and broadening of the Raman spectra, we carry out the integration of the equation (2) using the dispersion relation of linear diatomic chain gives by the eq. (4). To assess the quantum confinement effect in the Raman spectra by reducing the volume of quantum dots, the measured average diameter, was also included in the Richter line shape equation (2). Then a second integration with respect to L was carried out. F(L) is the log-normal distribution function obtained by fitting the histogram from AFM measurements.

$$F(L) = \frac{1}{\sigma} e^{-\left[\frac{\ln(L)-\ln(\bar{L})}{2\gamma^2}\right]} \tag{5}$$

Where $\bar{L}\ and\ \sigma$ are the mean diameter and width parameter, respectively. Eq. (5) allows introduce the diameter distribution of the QDots analytically into the Richter Raman line shape equation up (Eq. 2). Finally, the Ricther line shape then become

$$I(\omega, L) = I_0 \int_{BZ} \mathrm{F(L)I}(\omega)\mathrm{dL} \tag{6}$$

In order to analyze the broadening and asymmetry of the experimental Raman data, we used the model of three-dimensional phonon confinement. Raman spectra of InAs QDs were calculated using the equations (6), (4), and (3) and confinment function. In the Fig. 8, we show the result of our fitting for the experimental 290 cm^{-1} Raman band from samples M1-M4. In all fitting we only varied the intensity Io, the confinement parameter (σ) and 1/f Fano-parameter. The other parameters used in this fitting are show in the table 2. The spectra show a blue-shift of the LO GaAs mode, and an asymmetric broadening with decreasing QDs volume. We found that the phonon confinement model qualitatively explains the asymmetric lineshape and the increase in the FWHM with a decrease in the QDs volume. For the sample M1 with lower volume confinement, the spectrum calculated with the CM model differs considerably from the experimental data. By increasing the volume of confinement, (M2-M4 samples) the spectrum best fits the experimental data. Several authors report that the CM model explains very well the Raman spectra for nanocrystals (e.g. In or Ge QDs) with a diameter higher than 4 nm. This difference has been interpreted theoretically to be originated from the different crystallographic natures of their Raman spectra: crystalline for nonpolar and amorphous for polar nanosemiconductors. On the other hand, the wave function used in the quantum confinement model (CM) is of a single electron, and a single vibrational mode. However, in a finite crystal the vibrational modes depend on different values of the wave vector k_m [$k_m = \frac{m\pi}{Na} = \frac{m\pi}{L}$, m= 2,4,6,.... Max(a/D), where D is the diameter of crystallite], as a consequence of the boundary condition. In this case, an additional term is needed in the Eq. (6), but it is not the purpose of this work.

Table 2, shows the FWHM of the peak centered at 290 cm^{-1} (Fig. 7.); the mean height $\bar{L}$ ($\dot{A}$) and the FWHM obtained from fitting the AFM histogram with a log-normal distribution as shown in the inset of the Fig. 6. b.

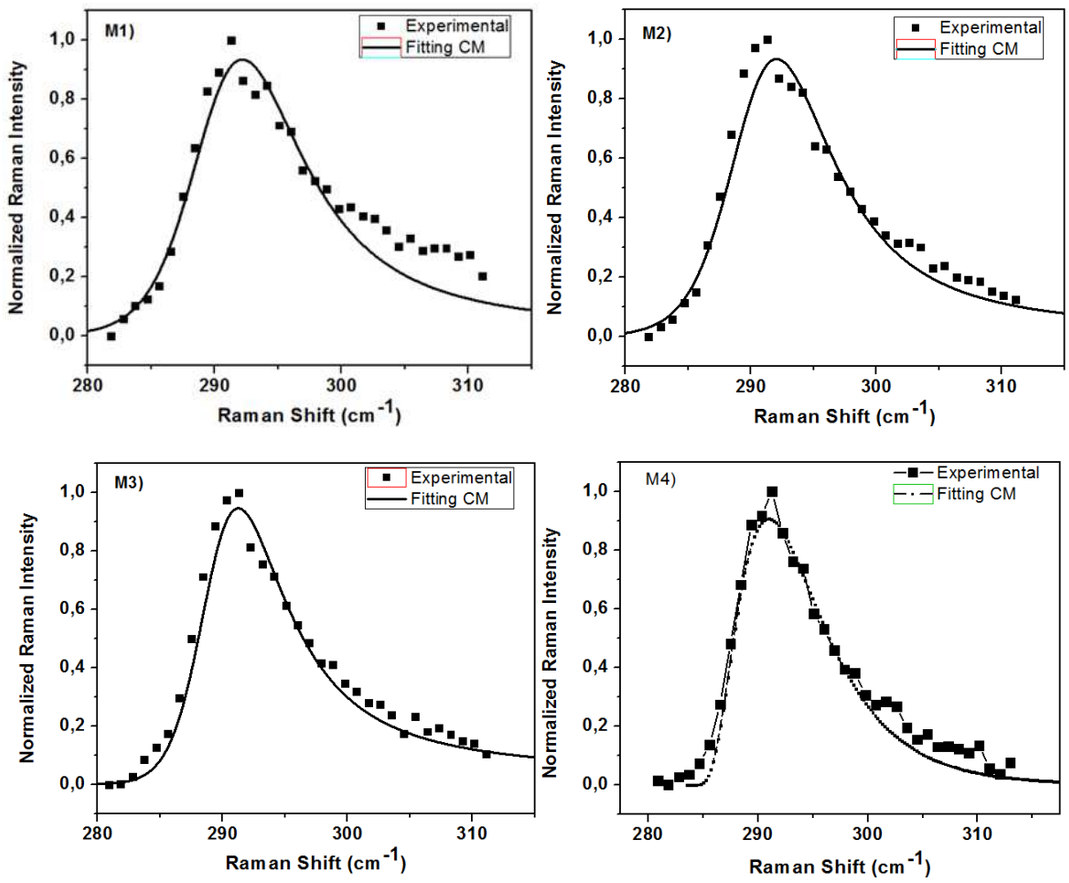

Fig. 8. Fitting on Raman spectra to the Confinement Model (CM). The square points are the experimental data and the continuous line is the CM by using the Eq(6).

Samples	FWHM Raman spectra (cm^{-1})	Mean height $\bar{L}$ ($\dot{A}$)	FWHM QDots distribution $\gamma(\dot{A})$
M1	9.8	17	35
M2	9.1	25	30
M3	9.0	30	24
M4	8.2	35	14

Table 2. Experimental data used to fit the Raman spectra

In the low frequency region of the LO phonon peak, we have observed a set of additional features in Raman spectra which can be associated to the SADQs (labeled by arrow, in Fig. 7., as known as *surface optical phonons* (*SO*). While phonons are collective lattice vibration modes, surface phonons are particular modes associated with surfaces; they are an artefact of periodicity, asymmetry, and the termination of bulk crystal structure associated with the surface layer of a solid [P. Nandakumara et al, 20001]. The SO-mode can be observed in the Raman scattering processes due to: a) impurity or interface imperfections, b) valence band mixing arising from the degeneracy at the Γ point in the Brillouin zone of zinc-blende semiconductors, and c) non-spherical geometry of the QDs. The study of surface phonons

provides valuable insight into the surface structure and other specific properties from the surface region, which often differ from bulk. Owing to the small size in QD's, the surface-to-volume ratio contribution to the Raman spectrum is much higher than in bulk crystals. In nanocrystals such as InAs QDots these modes can appear when the nanostructures are surrounded with a material of different dielectric constant ω(ε), e.g air (ε = 1). In large crystals, phonons propagate to infinity and the 1st order Raman spectrum only consists of q=0 phonon modes. When crystalline perfection is destroyed due to lattice disorder and defects, symmetry forbidden modes (like SO phonon modes) are activated and become stronger with increasing defect density. SO-phonon modes are localized to the interfase, and can propagate along the interface. They are solutions to Maxwell's equations with appropriate boundary conditions [B. E. Sernelius, 2001]. Many authors have studied theoretically the SO-modes from different geometries (cylindr ical and spheroids shape) in nanoparticles, nanowires and QDs, by using the approximation of a dielectric continuum and modeling of valence-force fields to explain the connection between SO phonon modes and the geometrical shape of a semiconductor QD [][Watt M et al, 1990; -37, Gupta R et al, 2203 -38].

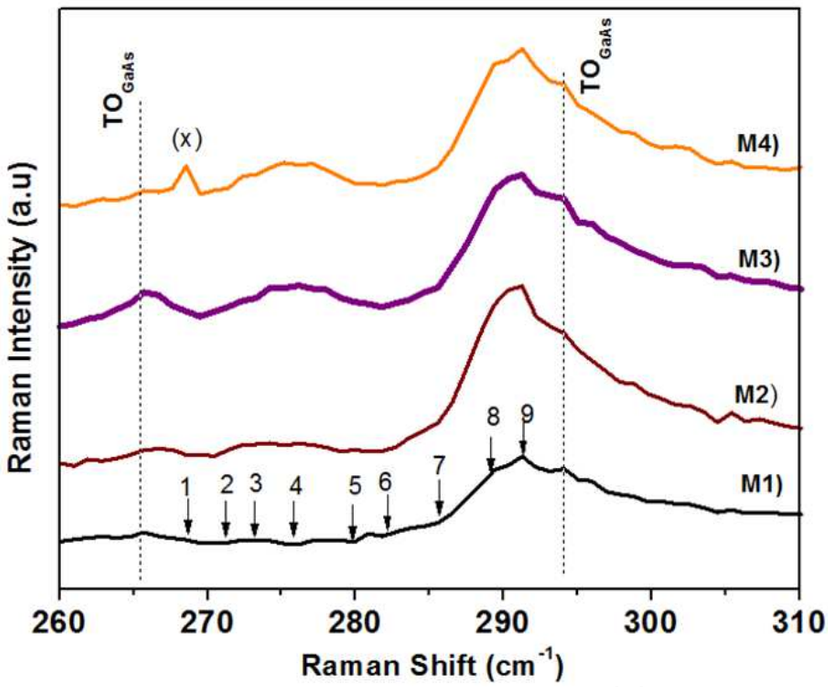

Fig. 9. Enlargement of the Raman spectra of the InAs SAQDs in the surface optical (SO) region. The arrows indicate small features related to the Rabi-type oscillations between two exciton levels. (x) in the sample M5 denote a phonon mode related to InAsN.

In our samples we observed that the integrated Raman intensity, and the position of the SO-mode for the samples M3 – M4 is clearly dependent of the volume and facets formed on SADQs. For sample M1 with quantum dots of smaller volume, and facets oriented along (113), a set of surface phonon modes indicated by a down-arrow (labeled from 1 to 9) are clearly identifiable. By increasing the confinement volume of quantum dots, M2 - M4 samples, (SO) phonon modes evolve in a continuum of states due to lowering of phonon

quantum confinement. We believe that the splitting of the phonon modes in this region probably is related to combined effect of SO-surface and exciton oscillating modes. Vasilevskiy *et al* [M. I. Vasilevskiy 2005], using a non-perturbative approach to calculate the multi-phonon resonant Raman scattering probability in semiconductor QDs, show that when inter-level coupling is strong, in the first order Raman spectrum appear features similar to those obtained in the electron spectral function, effect known as Rabi splitting [S. Hameau et al, 1999]. They correspond to the exciton oscillating between its two states and (many times) emitting and absorbing a phonon. The electron–phonon interaction is important in semiconductors and, especially, in semiconductor nanostructures since it determines hot carrier relaxation, influences light absorption and emission processes and is responsible for Raman scattering. The intensity of this interaction is enhanced in quantum dots (QD's) and, owing to the discrete nature of the electron energy spectrum, it leads to multi-phonon processes and formation of a polaron.

By comparing the position of SO-mode of the samples M2 and M3 (surrounded by air, $\varepsilon = 1$) with the nitrogenated M4- sample position (surrounded with N, $\varepsilon_N = 1.454$), we find an up-shift of 1.0 cm^{-1}. It is show a dependence of SO-mode with a systematic increase in the dielectric function that is surrounding the QDs. Further SO-modes, an additional peak (268.5 cm^{-1}, labelled (x)) from LO-InAsN phonon mode was only observed in the nitridated –M4 sample. In addition of the confined optic phonons, the presence of surface phonons in the Raman spectra of nanostructured of materials has been reported in a number of systems [Ingale A. et al, 1998; Alim et al, 2005]. Recently Ladanov et al [M. Yu et al, 2005] reported theoretical calculation of surface modes (SO) on spherical shape InAs QDs surrounded by a AlAs layer and air using the approximation of a dielectric continuum. They found that the frequencies of interface phonons (SO) obtained within this model lie in the spectral range between the frequencies of TO and LO phonons, and depend on the shape of the quantum dots.

On the other hand, in the region from 310 cm^{-1} to 500 cm^{-1} (Fig. 7.) we observed a set of peaks associated to electronic transitions. The Raman signal from electronic excitations in quantum dots is expected to be very small unless we can take advantage of some resonance mechanism. In order to enhance the resonance Raman signal, we used a laser with a energy (1.9 eV) very close to the $E_0+\Delta$ gap for InAs quantum dots (1.7 eV measured from PL resonant experiments by W. Dasilva *et. al*. [W. da Silva et al, 1997]). The energy difference between the electronic states which can be measured in Raman and FIR absorption spectroscopy is on the order of 50 meV. The first observation of electronic excitations in self-assembled QDs was reported by L. Chu and coworkers [L. Chu et al, 1997; L. Chu et al, 2000]. The sample studied contained 15 layers of InGaAs QDs, each layer having a n-type GaAs doping layer in its vicinity. The number of electron confined into each QD was estimated to be $N_e = 6$. By using an excitation laser at an energy of 1.71 eV very close to $E_0+\Delta$ gap, they found a peak at about 50 meV (403.2 cm^{-1}) in the depolarized Raman spectra, which was interpreted as a spin density excitation (SDEx) with a transition between the p and d level (with general quantum number N=2 and N=3) in the quantum dots. In our experimental resonant Raman spectra (Fig 6) we observed a similar peak located around of 46 meV (377.1 cm^{-1}) for the samples M3-M5 (with N) in well agreement with previous report. However, for the samples M1 and M2 with smaller QDs volume a set of Raman signal coming from electronic transitions was not observed, due to small number of electrons confined in quantum dots by reducing the confinement volume.

4. Conclusions

Self-assembled InAs(N) quantum dots were grown on GaAs (001) substrates by molecular beam epitaxy. We studied the variation in geometry and density of SAQDs for different growth temperatures. The average InAs dots size tends to increase whilst their density tends to decrease when the growth temperature is increased, possibly due to an increase in the surface mobility of In adatoms. We observed that the nitridation of InAs SAQDs starting from the wetting layer formation promoted the formation of quantum dots of larger dimensions.

5. Acknowledgments

This work was partially supported by CONACyT-Mexico, ICTDF-Mexico; DIMA and COLCIENCIAS-Colombia. The authors thank the technical assistance of R. Fragoso, A. Guillen, Z. Rivera, and E. Gomez

6. References

A. Pulzara-Mora, E. Cruz-Hernández, J. Rojas-Ramirez, R. Contreras-Guerrero, M. Meléndez-Lira, C. Falcony-Guajardo, M.A. Aguilar-Frutis, and M. López-López. (2007). Study of optical properties of GaAsN layers prepared by molecular beam epitaxy. *Journal of Crystal Growth*, Vol 301-302, (April 2007), pp. 565-569. doi:10.1016/j.jcrysgro.2006.11.241

A. Ueta, S. Gozu, K. Akahane, N. Yamamoto, and N. Ohtani. (2005). Growth of InAsSb Quantum Dots on GaAs Substrates Using Periodic Supply Epitaxy. *Japanese Journal of Applied Physics*, Vol. 44, (May 2005), pp. L696-L698, ISSN 0021-4922.

Adu K.W., Gutierrez H.R., Kim U.J., Sumanasekera G.U. & Eklund P.C. (2005). Confined phonons in Si nanowires. *Nano Lett.* 5, 409 , ISSN: 1530-6984

Alim K, Fonoberov V, Balandin. (2005). Origin of the optical phonon frequency shifts in ZnO quantum dots, *Appl. Phys. Lett.*; 86: (January 2005), p.p. 053103-3. ISSN 0003-6951.

B. E. Sernelius. (2001). *Surface Modes in Physics*, 1st edn. (Wiley-VCH, New York), p. 350. ISBN 3-527-40313-2

Benisty, H.; Sotomayor-Torres, C. M. & Weisbuch, C. (1991). Intrinsic mechanism for the poor luminescence properties of quantum-box systems, *Physical Review B*, Vol. (November 1991)) 44, p.p 10945–10948. ISSN 10945-10948.

Fauchet P.M. & Campbell I.H. (1988). Raman-spectroscopy of low-dimensional semiconductors. *Critical reviews in solid state and materials sciences* 14, p,p S79-101, ISSN: 0161-1593.

Gupta R., Xiong Q., Mahan G.D. & Eklund P.C., (2003). Surface optical phonons in gallium phosphide nanowires. *Nano Lett.*, 3, (Dec 2003), p.p 1745-50, ISSN: 1530-6984.

H. Lee, R. Lowe-Webb, W. Yang, and P. C. Sercel. (1998). Determination of the shape of self-organized InAs/GaAs quantum dots by reflection high energy electron diffraction. *Applied Physics Letters*, Vol. 72, No. 7, (February1998), pp. 812-814, ISSN 0003-6951.

Ingale A, Rustagi KC. (1998). Structural and particulate to bulk phase transformation of CdS film on annealing: A Raman spectroscopy study, *Phys. Rev., B*; 58: (October 2009), p.p. 7197-204.. ISSN 0021-8979.

J. Wu, W. Walukiewicz, K. M. Yu, J. W. Ager, III, E. E. Haller, Y. G. Hong, H. P. Xin, and C. W. Tu. (2002). Band anticrossing in GaP1-xNx alloys. *Physical Review B*, Vol. 65, No. 24, (June 2002), pp. 241303-241306, ISSN 1098-0121.

J.W. Lee, D. Schuh, M. Bichler, and G. Abstreiter. (2004). Advanced study of various characteristics found in RHEED patterns during the growth of InAs quantum dots on GaAs (0 0 1) substrate by molecular beam epitaxy. *Applied Surface Science*, Vol. 228, No. 1-4, (April 2004), pp. 306-312. ISSN 0169-4332.

L. B. Freund. Int. J. Influence of strain on functional characteristics of nanoelectronic devices. (2001). *Solids Struct.* 37 (august 2001) p.p 1925-1935. doi:10.1016/S0022-5096(01)00039-4.

L. Chu, A. Zrenner, M. Bichler, G. Böhm, G. Abstreiter. (2000). Raman spectroscopy of In(Ga)As/GaAs quantum dot. *Appl. Phys. Lett.* 77 (24), (october 2000), p.p 3944-3946. ISSN 0003-6951.

L. Ivanova, H. Eisele, A. Lenz, R. Timm, M. Dähne, O. Schumann, L. Geelhaar, and H. Riechert. (2008). Nitrogen-induced intermixing of InAsN quantum dots with the GaAs matrix. 92 (2008) 203101. *Applied Physics Letters*, Vol. 92, No. 20, (May 2008), pp. 203101-203103, ISSN 0003-6951.

M. Grujic - Brojcin, M.J. S. cepanovic, Z. D. Dohcevic-Mitrovic and Z.V. Popovic. (2009). *Acta physica polonica* A, Vol. 116, p.p 51-54. Proceedings of the Symposium A of the European Materials Research, Warsaw, September 2008.

M. I. Vasilevskiy and R. P. Miranda. (2005). Is polaron effect important for resonant Raman scattering in self-assembled quantum dots?. *phys. stat. sol. (c)* 2, No. 2, (February 2005), p.p 862–866. DOI 10.1002/pssc.200460352.

M. Sopanen, H. P Xin, and C. W. Tu. (2000). Self-assembled GaInNAs quantum dots for 1.3 and 1.55 μm emission on GaAs. *Applied Physics Letters*, Vo. 76, No. 8, (February 2000), pp. 994-996, ISSN 0003-6951.

M. Watt, C. M. Sotomayor Torres, H. E. G. Arnot and S P Beaumont. (1990). Surface Phonon Modes in GaAs Cylinders, *Semicond Sci Technol* 5, issue 4 (April 1990), pp. 285-290. ISSN 0268-1242.

M. Yu. Ladanov, A. G. Milekhin, A. I. Toropov, A. K. Bakarov, A. K. Gutakovskii, D. A. Tanne, S. Schultze, and D. R. T. Zahn. (2005). *Journal of Experimental and Theoretical Physics*, Vol. 101, No. 3, (april 2005) pp. 554–561. Origin: CROSSREF; ADS. DOI: 10.1134/1.2103225.

Osamu Suekane, Shigehiko Hasegawa, Toshiko Okui, Masahiro Takata and Hisao Nakashima. (2002). Growth Temperature Dependence of InAs Islands Grown on GaAs (001) Substrates. *Jpn. J. Appl. Phys.* 41 (November 2001) pp. 1022-1025. 10.1143/JJAP.41.1022.

P. Nandakumara, C. Vijayana, M. Rajalakshmib, Akhilesh, K. Arorab. (2001). Raman spectra of CdS nanocrystals in Nafion: longitudinal optical and confined acoustic phonon modes. *Physica E* 11, ISSUE No 4. 377–383. (November 2001), PII: S 1386-9477(01)00157-6.

R. Heitz, H. Born, F. Guffarth, O. Stier, A. Schliwa, A. Hoffmann, and D. Bimberg. 2001. Existence of a phonon bottleneck for excitons in quantum dots. *Physical review b*, volume 64, (November 2001), p.p. 241305-1 – 241305-4, ISSN:1098-0121.

Richter H., Wang Z.P. & Ley L. (1981). The one phonon Raman-spectrum in microcrystalline silicon. *Solid State. Commun*., 39, P.P 625-629, ISSN: 0038-1098.

S. Franchi, G. Trevisi, L. Seravalli, P. Frigeri. (2003). Quantum dot nanostructures and molecular beam epitaxy. *Progress in Crystal Growth and Characterization of Materials* 47 (April 2005) p.p. 166-195. doi:10.1016/j.pcrysgrow.2005.01.002. Available online 7 April 2005.

S. Hameau et al. (1999).. Strong Electron-Phonon Coupling Regime in Quantum Dots: Evidence for Everlasting Resonant Polarons, *Phys. Rev. Lett*. 83, (February 2995), p.p 4152 – 4155. ISSN 1089-7550.

S. Kiravitaya, Y. Nakamura, O. G. Schmidt. 2002. Photoluminescence linewidth narrowing of InAs/GaAs self-assembled quantum dots. *Physica E* 13, Volume 13, Issues 2-4 (January 2002), p.p 224-228 . ISSN 1386-9477.

S. O. Cho, Zh. M. Wang, and G. J. Salamo. (2005). Evolution of elongated (In,Ga)As–GaAs(100) islands with low indium content. *Applied Physics Letters*, Vol. 86, No. 11, (March 2005), pp. 113106-113108, ISSN 0003-6951(20050314)86:11;1-T.

T. Hanada, B. H. Koo, H. Totsuka, and T. Yao. (2011). Anisotropic shape of self-assembled InAs quantum dots: Refraction effect on spot shape of reflection high-energy electron diffraction. *Physical Review B*, Vol. 64, No. 16, (October 2001), pp. 165307-165312, ISSN 1098-0121.

T. Kita, Y. Masuda, T. Mori and O. Wada. (2003). Long-wavelength emission from nitridized InAs quantum dots. *Applied Physics Letters*, Vol. 83, No. 20, (November 2003), pp. 4152-4153, ISSN 0003-6951(20031117)83:20;1-Y.

T. Kudo, T. Inoue, T. Kita, and O.Wada. (2008). Real time analysis of self-assembled InAs/GaAs quantum dot growth by probing reflection high-energy electron diffraction chevron image. *Journal of Applied Physics*, Vol. 104, No. 7, (October 2008), pp. 074305-074309. doi:10.1063/1.2987469.

T. Matsuura, T. Miyamoto, T. Kageyama, M. Ohta, Y. Matsui, T. Furuhata, and F. Koyama. (2004). Elongation of Emission Wavelength of GaInAsSb-Covered (Ga)InAs Quantum Dots Grown by Molecular Beam Epitaxy. *Japanese Journal of Applied Physics*, Vol. 43, (January 2004), pp. L82-L84, ISSN 0021-4922.

Tomoyuki Sekine, Kunimitsu Uchinokura, Etsuyuki Matsuura. 2002. Two-phonon Raman scattering in GaAs. *Journal of Physics and Chemistry of Solids*. Volume 38, Issue 9 (September 2002),p.p 1091-1096. doi:10.1016/0022-3697(77)90216-5. Available online 23 September 2002

Ugo Fano (1961). Effects of Configuration Interaction on Intensities and Phase Shifts. *Phys. Rev*. 124, pp. 1866–1878. doi:10.1103/PhysRev.124.1866.

V. Sallet, L. Largeau, O. Mauguin, L. Travers, and J. C. Harmand. (2005). MBE growth of InAsN on (100) InAs substrates. *Phys. Stat. Sol.* (b) 242 (march 2005) R43 – R45. ISSN: 1521-3951.

W. da Silva, Yu. A. Pusep, J. C. Galzerani, D. I. Lubyshev, P. P. González-Borrero, and P. Basmaji(1997). Photoluminescence study of spin - orbit-split bound electron states

in self-assembled InAs and $In_{0.5}Ga_{0.5}As$ quantum dots. J. Phys.: Condens. Matter. 9, Issue 1 (January 1997), p.p L13-L17. doi:10.1088/0953-8984/20/35/354007.

W. Walukiewicz. (2004). Narrow band gap groput III-nitride alloys. *Physica E* 20, (March 2005), p.p 300 – 307, ISSN: 1386-9477.

IntechOpen

IntechOpen

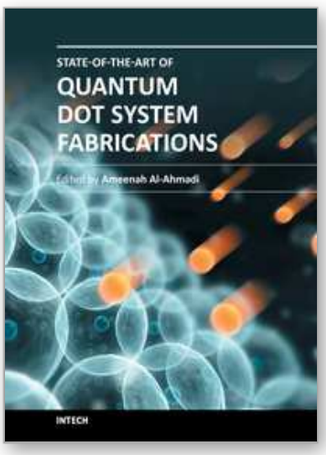

State-of-the-Art of Quantum Dot System Fabrications

Edited by Dr. Ameenah Al-Ahmadi

ISBN 978-953-51-0649-4
Hard cover, 172 pages
Publisher InTech
Published online 13, June, 2012
Published in print edition June, 2012

The book "State-of-the-art of Quantum Dot System Fabrications" contains ten chapters and devotes to some of quantum dot system fabrication methods that considered the dependence of shape, size and composition parameters on growth methods and conditions such as temperature, strain and deposition rates. This is a collaborative book sharing and providing fundamental research such as the one conducted in Physics, Chemistry, Material Science, with a base text that could serve as a reference in research by presenting up-to-date research work on the field of quantum dot systems.

How to reference

In order to correctly reference this scholarly work, feel free to copy and paste the following:

Alvaro Pulzara-Mora, Juan Salvador Rojas-Ramírez, Victor Hugo Méndez García, Jorge A. Huerta-Ruelas, Julio Mendoza Alvarez and Maximo López López (2012). Self-Assembled InAs(N) Quantum Dots Grown by Molecular Beam Epitaxy on GaAs (100)*, State-of-the-Art of Quantum Dot System Fabrications, Dr. Ameenah Al-Ahmadi (Ed.), ISBN: 978-953-51-0649-4, InTech, Available from: http://www.intechopen.com/books/state-of-the-art-of-quantum-dot-system-fabrications/self-assembled-inas-n-quantum-dots-grown-by-molecular-beam-epitaxy-on-gaas-100

INTECH
open science | open minds

InTech Europe
University Campus STeP Ri
Slavka Krautzeka 83/A
51000 Rijeka, Croatia
Phone: +385 (51) 770 447
Fax: +385 (51) 686 166
www.intechopen.com

InTech China
Unit 405, Office Block, Hotel Equatorial Shanghai
No.65, Yan An Road (West), Shanghai, 200040, China
中国上海市延安西路65号上海国际贵都大饭店办公楼405单元
Phone: +86-21-62489820
Fax: +86-21-62489821

© 2012 The Author(s). Licensee IntechOpen. This is an open access article distributed under the terms of the Creative Commons Attribution 3.0 License, which permits unrestricted use, distribution, and reproduction in any medium, provided the original work is properly cited.

IntechOpen

IntechOpen